TECHNICAL MEMORANDUMS

NATIONAL ADVISORY COMMITTEE FOR AERONAUTICS

No. 879

STATIC LONGITUDINAL STABILITY AND LONGITUDINAL CONTROL OF AUTOGIRO ROTORS

By M. Schrenk

Luftfahrtforschung
Vol. 15, No. 6, June 6, 1938
Verlag von R. Oldenbourg, München und Berlin

Washington
October 1938

NATIONAL ADVISORY COMMITTEE FOR AERONAUTICS

TECHNICAL MEMORANDUM NO. 879

STATIC LONGITUDINAL STABILITY AND LONGITUDINAL CONTROL OF AUTOGIRO ROTORS*

By M. Schrenk

SUMMARY

The present report discusses three different systems of elevator control and their effects on the stability and maneuverability of autogiros: (a) ailerons and elevators (standard); (b) blade control (la Cierva); (c) gravity control (new).

The control sensitivity $\frac{dv}{d\beta}$, which is dependent to a great degree on the speed in system (a), becomes substantially more uniform in system (b), and practically constant through the whole range from zero to maximum speed in system (c). At the same time, the highest restoring moments attainable at pull-up become consistently smaller. The important characteristics of blade control and gravity control are:

1) Flattening out from a high-speed dive is smoother and with little stress;

2) The airplane can be landed with very small control deflections;

3) Steering is not too sensitive at high speeds;

4) The maximum permissible speed can be easily and safely limited by control movements, a fact which constitutes a special safeguard for an autogiro rotor having a prescribed maximum coefficient of advance.

The control-force balance can be readily achieved by proper design of the rotor head with its suspension. The

*"Statische Längsstabilität und Höhensteuerung von Tragschrauben." Luftfahrtforschung, vol. 15, no. 6, June 6, 1938, pp. 283-289.

control forces (to be kept moderate) with blade control and gravity control also change linearly with the speed. The shifting of the equilibrium condition or balance of center of gravity displacements, attainable by suitable structural design of the rotor head assembly, affects neither stability nor control-force variation.

I. INTRODUCTION

1. Aerodynamic Principles

1) The calculation of the rotor-blade moments is apparent from the report entitled "The Aerodynamic Principles of the Autogiro Rotor" (reference 1). In it the flow losses at the rotor had been divided into three sections, characterized by the three coefficients ϵ_l, ϵ_d, and ϵ_u. It was proved that the resultant rotor force at vanishing coefficient of advance must, for reasons of symmetry, lie in the axis of rotation and that the asymmetrical inflow of the rotor of finite coefficient of advance is followed by a backward inclination of the resultant in relation to the axis of rotation.

In figure 1, accordingly, the total force (S) of the "rotor of vanishing coefficient of advance" is located in the axis of rotation (dash-dots), the actual resultant S is further inclined by ϵ_u; ϵ_u is the coefficient of the nonuniformity loss. The result is the plot of figure 2, upon which the entire subsequent calculation of the rotor moments is based. The end points of the rotor force vectors (coefficient c_s) are approximately located (as is readily proved) on a parabola of the second order.

Admittedly this is applicable for the present only to the simplified picture of an autogiro rotor with very heavy blades, where the blades, sufficiently approximated, may be visualized as rotating in one plane. The 6° to 9° cone angles for the conventional blade designs cause a certain forward shift of the air forces, especially at small angles of attack. It further is assumed that the blade hinges lie in the axis of rotation. But in reality they are always a certain distance away from it for constructional reasons.

Both effects enhance the stabilizing actions of the air forces on the rotor moment, but, being little amenable to mathematical treatment, will be disregarded here. The

stability of actually constructed autogiro rotors is somewhat higher, the control action a little less than that computed with the simplified assumptions.

Likewise, we disregard the lateral inclination of the resultant, as consequence of the cone motion and curvature of the flow. The arguments are wholly restricted to the plane of symmetry.

2) The problem of downwash on the tail group is much less cleared up. Theory fails to yield anything comprehensible; measurements are nonexistent. Hence a plausible assumption must be found. The slope of the downwash must be associated with the induced angle of attack α_i, which indicates the slope of a plane substitute flow at the rotor. In first approximation the slope of downwash will be proportional to α_i. The ratio must, for lack of data, be estimated in accord with the position of the tail relative to the rotor.

This, undoubtedly, is the most questionable factor of the whole calculation, although the effect of an eventual error will not alter the results materially.

2. Procedure

The method of calculation is fundamentally the same as in the usual static stability studies.

The rotor moment is built up from the share of the air forces and that of the centrifugal forces by eccentric blade hinges. The latter effects a displacement of the moment lines and is easily computed on the assumption of quasi-stationary condition. The tail moment affords no straight lines because of the nonlinear relation between α and c_s.

The two moment quotas can be combined in various ways, depending upon the control design. The following three systems are examined:

a) Ailerons and elevators as on normal airplane: wing fixed at body, tail surfaces hinged.

b) Blade control: tail surfaces fixed on body, rotor movable about a transverse axis located in the hub;

c) Gravity control: rotor and tail movable simultaneously and equably, and producing a c.g. displacement.

The result is a set of total-moment curves of very different character. The magnitude of attainable stability can be expressed with $\frac{d\ c_m}{d\ \alpha}$. The control action is represented by a comparative quantity proportional to the flying speed plotted against the control (or rotor) deflection β, respectively. It results in pronounced fundamental differences between the three systems.

This is followed by the determination of the control forces over the speed for the case of movable rotor and a discussion of the means for attaining different trims.

3. Fundamental Data

The basic assumptions, resembling the conditions of actually constructed gyroplanes, are as follows:

Solidity	$\sigma = 0.10$
Profile drag coefficient of blade	$c_{w_p} = .01$
Blade angle	$\vartheta = 1.8^\circ$

for which the formulas (of reference 1) give the characteristic quantities of the autogiro* as

Coefficient of axial flow	$\lambda_d = 0.021$
Thrust	$k_s = .012$
Coefficient of flow	$\zeta = .19$

The pertinent relationship between air-force factor c_s and angle of attack α is illustrated in figure 3.

The other dimensions will be found in the cited report. Ratios were introduced wherever possible; where this was impractical a light two-seater of 600 kg gross weight and 10 m rotor-blade diameter served as basis.

*According to those formulas (III, 11)(III, 15) and (III, 17), the quantities are computed at $c'a_p = 5.6$ for the rectangular blade.

4. Symbols

Other than the symbols given in the cited report (reference 1) the following are also used:

r	c.g. position back
h	height of rotor position
l_H	tail surface lever arm
a, b, c, d, e, f	dimensions of control according to figure 17
m	mass of rotor blade per unit length
p	proportionality factor for downwash slope
β	angle of the control (β_H, β_F)
P	control-stick force

II. Partial Moments

1. Rotor Moment, Hinges in Axis of Rotation

With the notation of figure 4 (where the backward position r of the center of gravity is negative) the air-force moment S is:

$$M_S = - S(h \epsilon_u + r)$$

which, reduced to dynamic pressure, rotor area, and diameter, gives the moment factor

$$c_{m_S} = \frac{M_S}{\rho/2 \; v^2 \; F \; D} = - c_s \frac{h}{D} \left(\epsilon_u + \frac{r}{h} \right)$$

According to the report 345 (reference 1), ϵ_u can be expressed in the fundamental quantities of the autogiro. With $\kappa = \frac{1}{8}$ and $\cos \alpha = 1$ (reference 1, formula VI, 9) for the lancet-shaped blade) it is:

$$\epsilon_u = \kappa \lambda = \frac{\lambda}{8} = \frac{\cos \alpha}{8} \sqrt{\frac{k_s}{c_s}} = \frac{1}{8} \sqrt{\frac{k_s}{c_s}}$$

Hence:

$$c_{m_s} = -c_s \frac{h}{D} \left(\frac{1}{8} \sqrt{\frac{k_s}{c_s}} + \frac{r}{h} \right) \qquad (1)$$

A general examination of figure 4 discloses that, with suitably chosen r, the rotor moments afford a stable equilibrium. The backward-position limit is r = 0 (c.g. in axis of rotation), whereby the rotor moment is balanced in vertical ascent; as the c.g. is shifted forward (r negative) the rate of the moment equilibrium increases.

The dotted lines (fig. 5) confirm this and indicate that fairly small c.g. displacements suffice to produce pronounced changes in the angle of attack of the balance. (To avoid decimal fractions, the moment coefficients are multiplied by 100.)

2. Rotor Moment, Hinges Eccentric

As already stated in the introduction, the effect of the blade-hinge distance from the axis of rotation is to be examined only as regards the moments of the centrifugal forces due to the flapping motion.

Figure 6 illustrates a rotor head with two hinges in the plane of symmetry. Under the initial assumption of the blades rotating in one plane, the centrifugal forces Z applied at the hinge are parallel and inclined through flapping angle β_1, the amount of which can be approximated (reference 1, IV, 10; factor $\frac{1}{\left(1 - \frac{\lambda^2}{2}\right)}$ is made = 3/2) at:

$$\beta_1 = 3\left(\lambda_d + \frac{4}{3}\vartheta\right)\lambda \qquad (2)$$

Now, an autogiro usually has three rather than two blades, and consequently two blade forces inclined $\pm 60^0$

toward the plane of symmetry instead of the one shown. The minor fluctuations in the resultant centrifugal forces occurring during rotation with six times the frequency of the revolution speed, in the plane of symmetry, can be ignored here.

Then, with m as the blade mass per unit length, we have:

$$Z = m\,\omega^2 \int_0^R r\,d\,r = \frac{1}{2}\,m\,u^2 = \frac{1}{2}\,m\,\frac{v^2}{\lambda^2}$$

$$M_z = -2Z\,a\,\beta_1$$

whence, with equation (2) and $\lambda = \sqrt{\frac{c_s}{k_s}}$

$$M_z = -3\,a\,m\,v^2\left(\lambda_d + \frac{4}{3}\,\vartheta\right)\sqrt{\frac{c_s}{k_s}}$$

and

$$\frac{M_z}{\rho/2\ v^2\ F\ D} = c_{m_z} = -\frac{\dot{o}}{\rho}\,\frac{m}{F}\,\frac{a}{D}\left(\lambda_d + \frac{4}{3}\,\vartheta\right)\sqrt{\frac{c_s}{k_s}} \qquad (3)$$

Regarding this deviation, it should be observed that the flapping angle β_1 in equation (3) is dependent on λ, c_s respectively. This formula therefore gives the additional moment due to the centrifugal force for the steady stage, that is, the dynamic pressure of horizontal flight for the related flight condition. In reality the dynamic pressure does not change at all in first approximation during angle of attack fluctuations; the moment of the centrifugal force, viewed from the momentary equilibrium condition, varies somewhat differently. To allow for this, it would be necessary to draw a second curve of the additional moments produced during oscillations from every point of the stationary curve. However, since it usually involves only small oscillations, this task is unnecessary, particularly within the scope of the present, strictly static analysis.

For the mathematical interpretation of equation (3), it should be borne in mind that m, the blade mass per

length, should be proportional to the disk area F, when c_{m_z} became unaffected by the scale. Now, $\frac{m}{F}$ is, without a doubt, not constant,* but bound to the scale; that is, definite numerical conditions must be used as a basis.

In conformity with the conditions on a light two-seater, assume

$D = 10$ m $\qquad F = 78.5$ m^2

$a = 80$ mm $\qquad mg = 2$ kg/m

The theoretical values are included in figure 5. They apply with slight changes to any other not abnormally different dimension.

3. Tail Moment

The angle of attack of the tail is according to the introduction and to figure 7:

$$\alpha_H(c_s) = \alpha(c_s) - p\ \alpha_i(c_s) + \beta_H \qquad (4)$$

The proportional factor p, which indicates the amount of slope of the flow at the tail as a result of its curvature over that at the rotor axis, is probably not altogether constant. But, lacking more exact information, a linear relationship is assumed for which $l_H/D = 0.5$, we put

$$p = 1.2$$

The tail with the deflection β_H is assumed to be undivided, in order to simplify the analysis.

In formula (4) $\alpha_i(c_s)$ is linear, while $\alpha(c_s)$ contains a parabolic share (angle of flow α_d, reference 1).

---

*To illustrate, if, by enlargement of the rotor the cone angle is to remain constant, the thrust load per unit length of blade increases at equal c_{a_p} and $\frac{G}{F}$ (u = const.) linearly with the diameter D, that is, the same must hold for radial loading. But this depends under the cited conditions, only on m, which in consequence itself increases linearly with D.

In consequence, $\alpha_H(c_s)$ will no longer be linear, that is, the tail-moment line is not straight.

Its coefficient is:

$$c_{m_H} = \alpha_H \, c'a_H \frac{F_H}{F} \frac{l_H}{D} \qquad (5)$$

$c'a_H$, the slope of the tail lift above its angle of attack, is for an aspect ratio of $\Lambda = 3$ (in degree):

$$c'a_H = \frac{0.055}{0.565 + 1/\Lambda} = 0.06^0$$

Since the rotor moment with suitably chosen c.g. position itself is stable, the choice of tail dimensions is merely contingent upon the desired control range and the necessary damping capacity against oscillations.

With the chosen proportionality factors

$$\frac{F_H}{F} = 1/100 \text{ and } \frac{l_H}{D} = \frac{1}{2}$$

equation (5) finally gives

$$100 \, c_{m_H} = 100 \, \alpha_H \times 0.06 \times 0.01 \times 0.5 = 0.03 \, \alpha_H(c_s)$$

When computing α_H according to equation (4), $\alpha(c_s)$ should be taken from figure 3, $\alpha_1(c_s)$ from figure 18 of Report No. 345 (reference 1). The obtained moment coefficients are shown in figure 8. The lines for different elevator deflections β_H differ from one another only by a constant difference in c_{m_H}.

III. TOTAL MOMENTS, STATIC STABILITY

1. Aileron and Elevator Control

The first case is that of the normal airplane control

and is treated as such. Figure 9 illustrates the somewhat more finely divided tail moments in comparison with the rotor moment for 0.02 backward c.g. position. Figure 10 gives the total-moment lines as algebraic sum of the partial moments. The course of these moments is not essentially different from that of the orthodox airplane. The control action $\frac{d\beta_H}{d\alpha}$, referred to angle of attack, in particular, is noticeably constant.

Instead of referring the control effect to the angle of attack, it is more practical to refer it to the speed. Figure 3 serves for the change from α to v, the curve $\frac{1}{\sqrt{c_a}} = k\,v$ presents a speed criterion.

The result of this conversion is shown in figure 11. The control response $\frac{dv}{d\beta_H}$ is very small at low speed and rises abnormally as v increases. In this respect the behavior of the tail-controlled autogiro is essentially the same as that of the orthodox airplane.

2. Blade Control

Instead of changing the equilibrium condition through deflections of the tail, the same effect, with fixed tail can be obtained by swiveling the rotor hub about a horizontal axis. The initiative of this avenue of attack followed by de la Cierva for several years was probably due to the desire of extending the flight range up to 90° angle of attack, that is, attain controlled vertical descent.

The effects of swiveling the axis by $\Delta\beta_F$ are directly observable from figure 4:

a) The backward c.g. position r is changed by the amount of $h\Delta\beta_F$: different blade moment.

b) The tail-setting angle - which always shall refer to the axis of rotation - is changed to the amount of $-\Delta\beta_F$ as a result of the setting: a different tail-plane moment.

As to a) a one-percent change in $\frac{r}{h}$ is equivalent to a turn of $\Delta \beta_F$ through ~ 0.6°. The figures of the blade-control angle β_F in figure 12 refer to the line connecting blade center to center of gravity; elsewhere, however, the axis of rotation remains the reference line for the angles of attack of rotor and tail.

Assume, for the blade moment, that the blade-control angle β_F in the normal flight range remains, say, between -0.5° and -2.5° (measured backward from the c.g.). The problem then is to find a set of tail plane curves which give, at the α_H defined by the setting, the moment equilibrium within the questioned range.

This problem is readily solved by selecting from the existing tail-plane moments (fig. 8) computed for $\frac{F_H}{F} = \frac{1}{100}$ a suitable line and so distorting its ordinate through a change of the ratio $\frac{F_H}{F}$ that the required set can be developed from the new curve. For example, the curve for $\beta_H = -3.1°$ from figure 8 is chosen, the ordinates reduced to $\frac{3}{5}\left(\frac{F_H}{F} = \frac{1}{120}\right)$ and then the new tail lines related to $\beta_F = -0.6°$ to $-2.4°$ determined by shifting through -0.6° each (fig. 12). These tail moments balance the rotor moments at the points indicated by the double arrows.

The resultant moments are shown in figure 13. Their character is substantially unlike that of the standard control system: $\frac{-\beta_F}{d\ \alpha}$ has long ceased to be constant.

The negative moments themselves do not reach such high values, as a result of which the take-off process will be smoother.

The control sensitivity $\frac{d\ v}{d\ \beta_F}$ is illustrated in figure 14. The (v, β_F) line is substantially flatter, i.e., the sensitivity with blade control fluctuates considerably less than with the standard system of control. This is an

unexpected and very propitious effect of the blade control.

3. Gravity Control

However, one may go a step farther. With the blade control, two effects occurred simultaneously: a change in rotor moment due to relative c.g. displacement and the change in tail moment due to the setting.

Now, the effect of the setting can be eliminated altogether, thus leaving only the c.g. displacement, by swinging the tail plane for the same amount as the rotor axis of rotation. This preserves the same angle relative to the axis of rotation.

The tail-plane moments are then indicated by one line, which effects a considerable simplification in the choice of the correct tail-plane dimensions and setting. The curve drawn in figure 15 is for a surface ratio of $\frac{F_H}{F} = \frac{1}{200}$ with fixed setting relative to the axis of rotation of $\beta_H = 0^\circ$. The reason of the much smaller tail area is due to the fact that the destabilizing effect of the varying setting has been removed.

The total moments are shown in figure 16. The negative moments are even smaller than with the blade control, hence the take-off will be still smoother. The small moment factors at small α should cause no concern since the absolute values are still fairly large as a result of the related high dynamic pressure. Still, they never will be so high that the airplane "jumps" when pulling the control quickly.

Aside from that, there is the practically linear control response obtainable only with gravity control (fig. 14). Such a variation of the (v, β_F) curve assures an airplane on which the absolute speed change is proportional to the control deflection! The large sensitivity differences of all airplanes with orthodox control surfaces and which even prevail to some extent in the blade-controlled autogiro are practically nonexistent with gravity control. Landings can be made with moderate control movements and steering is not too sensitive at high speeds. It also is possible forthwith to limit the attainable top speed by

control deflection, which is of especially great importance on the autogiro rotor designed for a certain maximum coefficient of advance.

It might be remarked that the preservation of a fixed angle between blade axis of rotation and control surfaces, or as it is called here, "gravity control" is simply a special case of positive connection of these two airplane parts. The gravity control may be "close" or "excessive," depending upon the choice of gear ratio. With "excessive" control, so that the control surfaces are still subject to an additional rotation in the same direction as the angular motion of the axis of rotation, it is directly conceivable to let the control sensitivity at a certain top speed drop to zero, i.e., to restrict the speed even more effectively than with "pure" gravity control. Naturally, it is then not easy to maintain the stability sufficiently high. It is also possible to work with differential effect between blade and control surfaces. In any case, this combination affords great freedom in the choice of the desired longitudinal control charactoristics.

IV. CONTROL FORCES

There remains yet the problem of control forces, and especially that of control balance, since it involves a large rotor rather than a small control. To be sure, the success of the Cierva type C 30 and CL 10 has shown that no fundamental difficulties exist, but the explanation of the numerical conditions is also of interest.

1. Force Balance

The chosen rotor control system must be primarily so designed that the control force at any flight stage (speed) passes through zero (stability with control released). Such an arrangement of "rotor head" is shown in figure 17. The horizontal axis of rotation (x) must be far enough ahead of the total air force S so that the ensuing nose-heavy moment of S balances the tail-heavy Z-moment. This equilibrium is stable with properly chosen dimensions, as is readily determinable. If in the place of the blade height h (fig. 4), the axial distance b and in place of the backward position r the distance c is introduced, the relations for the blade moment developed in a previous

chapter can be simply taken over. The moment about point x is expressed conformably to equations (1) and (3) by the coefficient

$$c_{m_x} = -c_s \frac{b}{D}\left(\frac{1}{8}\sqrt{\frac{k_s}{c_s}} + \frac{c}{b}\right) + c_{m_z} \qquad (6)$$

Let $\frac{b}{D} = \frac{1}{20}\frac{h}{D}$, according to equation (1); then the moments through S would be, if the amount of $\frac{c}{b}$ were chosen corresponding to $\frac{r}{h}$, small against c_{m_z}, which does not change relative to equation (3); that is, $\frac{c}{b}$ must be substantially higher than $\frac{r}{h}$.

The numerical value is contingent upon the chosen flight stage (α, c_s), in which equilibrium is desired. It is obtained from equation (6) as:

$$\frac{c}{b} = -\frac{1}{8}\sqrt{\frac{k_s}{c_s}} + \frac{c_{m_z}}{c_s}\frac{D}{b} \qquad (7)$$

The choice is a = b = 80 mm.

Further, let balance be desired at:

$$\alpha = \left\{\begin{matrix} 4.4^\circ \\ 7.2^\circ \\ 18.6^\circ \end{matrix}\right\} \text{ equivalent to } c_s = \left\{\begin{matrix} 0.07 \\ .15 \\ .6 \end{matrix}\right\}$$

for this equation (7) gives as control force balance:

$$\frac{c}{b} = \left\{\begin{matrix} -0.32 \\ -.22 \\ -.11 \end{matrix}\right\} \quad \text{or} \quad c = \left\{\begin{matrix} -25.5 \\ -17.5 \\ -9 \end{matrix}\right\} \text{ mm}$$

2. Control Forces

With these amounts of $\frac{c}{b}$, c_{m_x} can be computed from equation (6). But for changing to actual control forces,

the transmission ratio between control stick and blade as well as the stick length is needed. Suppose the total deflections are:

$$\Delta \beta_F = 3^\circ \text{ (fig. 14)}, \quad \Delta \beta_{st} = 48^\circ$$

that is, a 1:16 ratio between blade and control stick. This gives by way of example

$$d = 320 \text{ mm}, \qquad e = 20 \text{ mm}$$

Let the length of control stick be

$$f = 500 \text{ mm}$$

Then the control force becomes:

$$P = \frac{e}{d} \frac{D}{f} c_{m_x} q F$$

or, with $q = \frac{G}{F c_s}$

$$P = \frac{e}{d} \frac{D}{f} \frac{c_{m_x}}{c_s} G \tag{8}$$

which for $G = 600$ kg and $D = 10$ m finally affords

$$P = 750 \frac{c_{m_x}}{c_s}$$

The related numerical values are presented in figure 18. The point for $v = 0$ (vertical descent) is computed from the simple equilibrium equation (fig. 17):

$$M_x = c G$$

$$P = \frac{c}{d} \frac{e}{f} G = 0.075 c$$

All points are located on a straight line for a certain equilibrium stage ($c = \text{const.}$). Angles and forces at the control thus pass (at least with gravity control) to both

sides of the equilibrium speed, linearly with the speed change. The conceivably most promising longitudinal control characteristics are the result. The forces remain within ±2 kg, that is, easily applied.

3. Trim

A final problem involves the change - with blade or gravity control - of the equilibrium position with control released and the balancing of a displacement in the c.g. position.

1) The use of springs might be resorted to for influencing the equilibrium position. But they have the undesirable quality of forming vibratory systems. But there is one almost "natural" solution which consists (fig. 19) in mounting the pivot B adjustable in relation to the elevator lever C, so that the distance of the axis of rotation from the elevator axis (c in fig. 17) can be changed at will. Since it involves a space of a few mm only, this should be constructively easy (spindle with flexible shaft). Figure 18 presents the effect of the distance c on the equilibrium speed of our example.

2) The blade moment with wings fixed to the fuselage is very sensitive to c.g. displacements (fig. 5). With movable wings and stable stress distribution the c.g. displacement for control released is, of course, without effect on the blade moment, since it always assumes the same angle of attack to the air stream. But with blade control, the position of the body affects the setting between fin and blade, the fin receives an additional stress with the result that the stability is changed in unpredictable manner.

This is not the case with pure gravity control, because the angle of setting is not affected by the position of the fuselage. Still the changed position may have disagreeable consequences in practical service; the control stick setting for a certain flight condition in particular, changes when the c.g. is displaced. This might be overcome, by adjusting the push-rod length between control and blade; but it is more logical to simply shift the blade by the amount of the c.g. change relative to the fuselage. Figure 19 illustrates this with the carriage guide between D and E.

Such a solution results in an airplane on which changes

in equilibrium-dynamic pressure can be attained and center of gravity displacements can be balanced in a large measure, without one precautionary measure influencing the other or changing the static longitudinal stability of the whole system.

Translation by J. Vanier,
National Advisory Committee
for Aeronautics.

REFERENCE

1. Schrenk, Martin: Aerodynamic Principles of the Direct Lifting Propeller. T.M. No. 733, N.A.C.A., 1934.

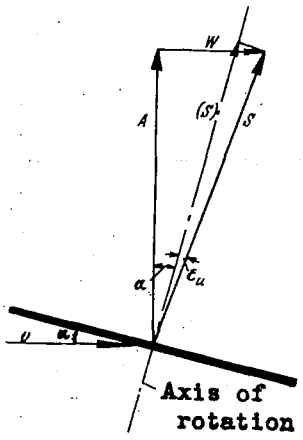

Figure 1.- Forces and angle at rotor blade.

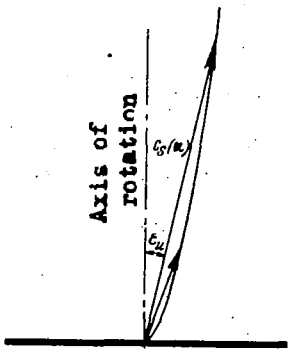

Figure 2.- Parabolic relationship between c_s and ϵ_u .

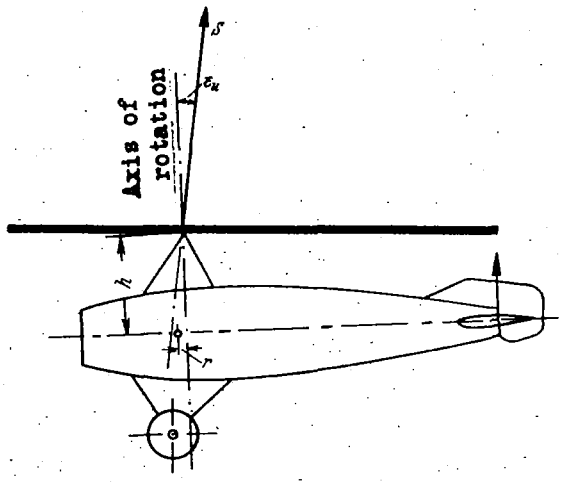

Figure 4.- Dimensions for defining the blade moment.

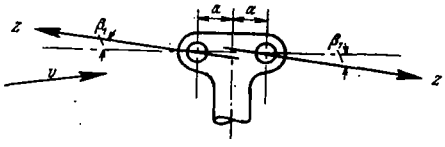

Figure 6.- Eccentrically applied centrifugal forces of the blades.

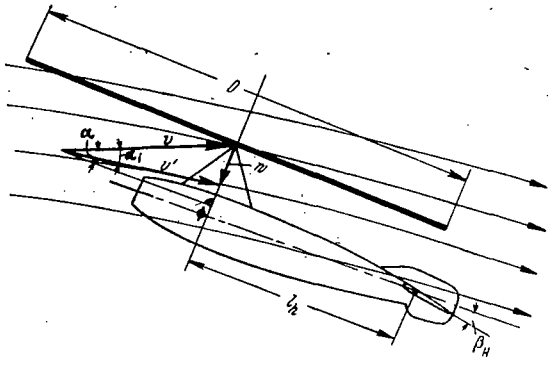

Figure 7.- Source of downwash at elevator control.

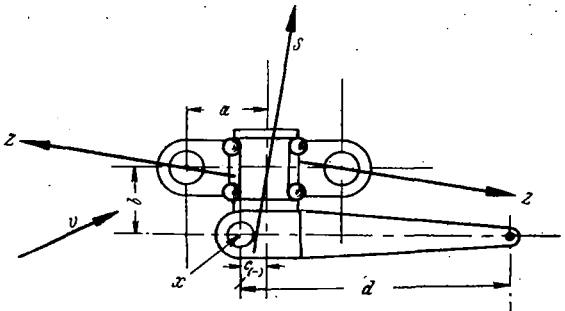

Figure 17.- Schematic drawing of rotor blade hub with elevator control.

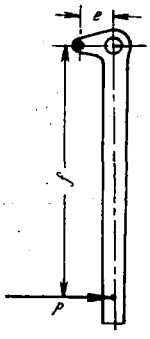

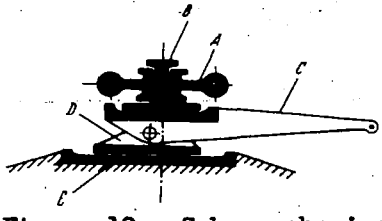

Figure 19.- Scheme showing arrangement for correct change in balancing condition and trim.

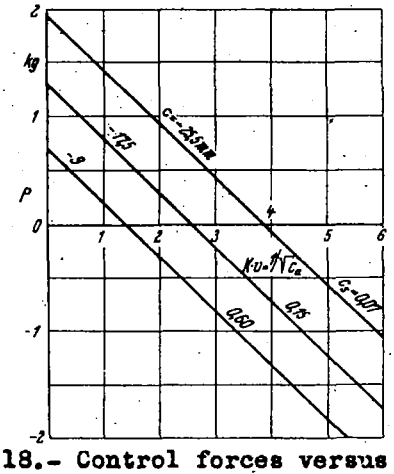

Figure 18.- Control forces versus speed for different balancing stages.

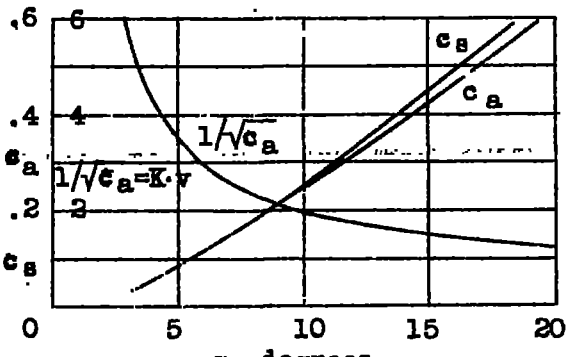

Figure 3.- Relationship between angle of attack and air force for the described example.

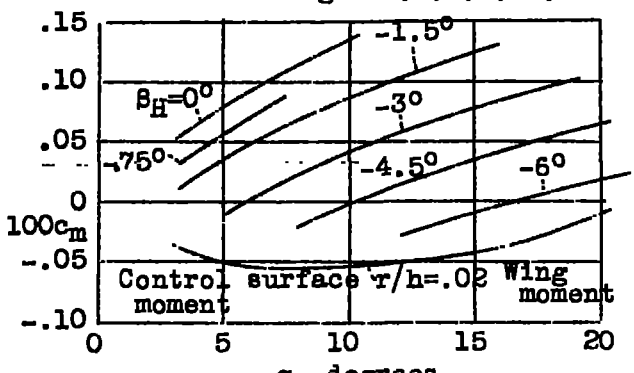

Figure 9.- Wing and tail moments for standard control system.

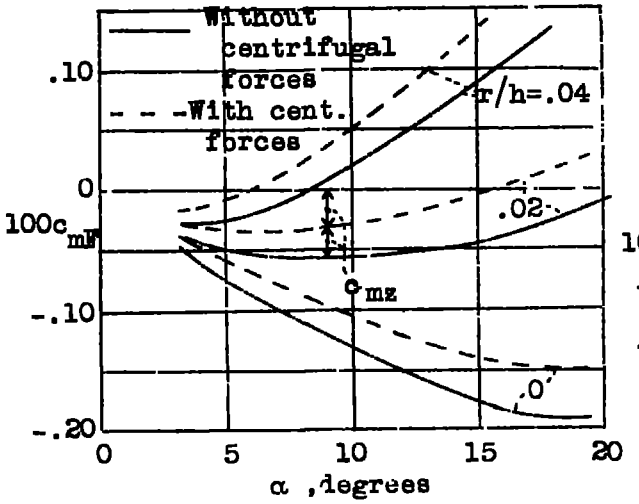

Figure 5.- Blade moments without and with centrifugal forces.

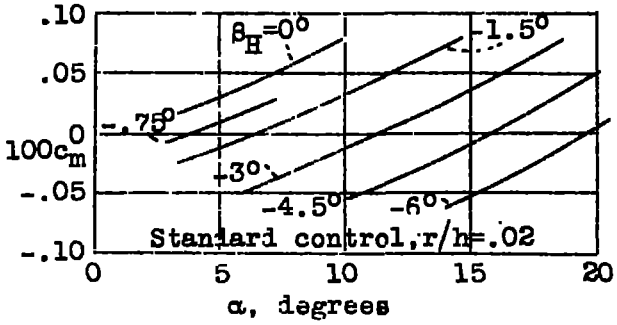

Figure 10.- Total moments for standard control system.

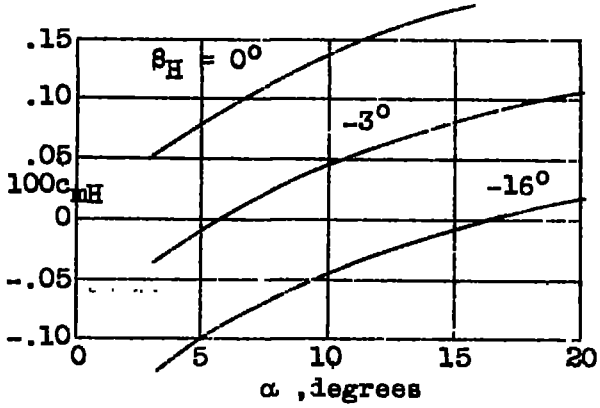

Figure 8.- Elevator moments.

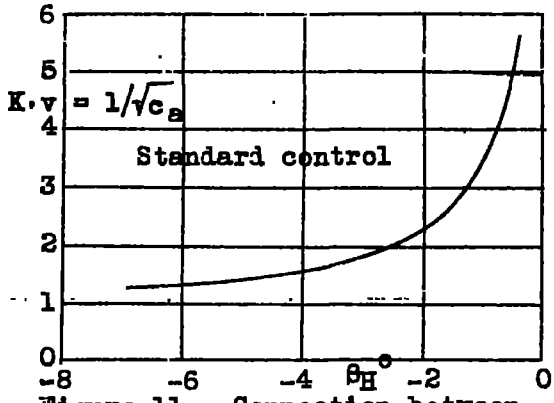

Figure 11.- Connection between speed and control deflection in standard control system.

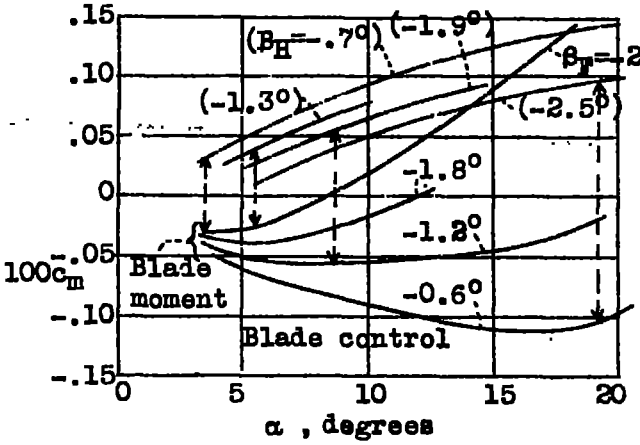

Figure 12.- Blade and control surface moments for blade control. The double arrows indicate the related lines and the point of the corresponding moment balance.

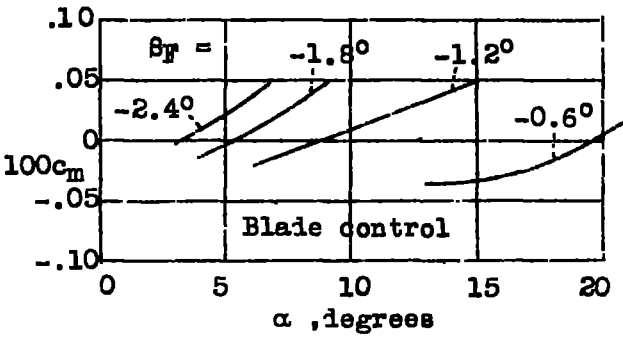

Figure 13.- Total moments for "blade control".

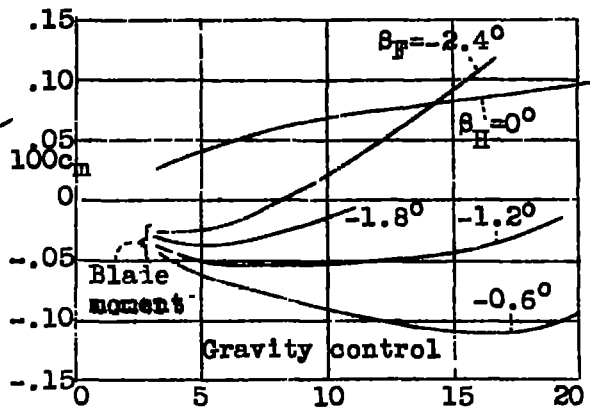

Figure 15.- Blade and control surface moments with "gravity control".

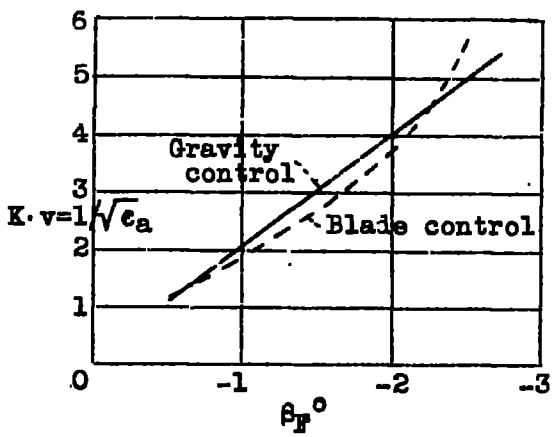

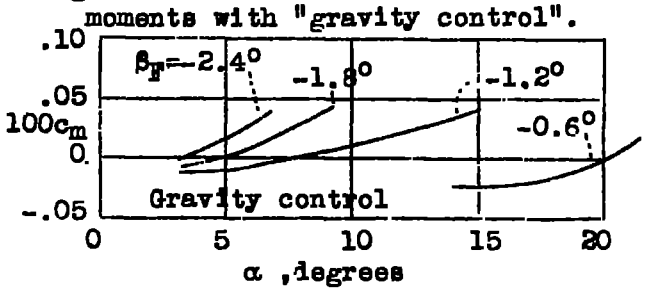

Figure 16.- Total moments with "gravity control".

Figure 14.- Relation between speed and control deflection for "blade control" and "gravity control". The control sensitivity corresponds to the slope of the tangent to the curve at the particular point, it is practically constant with "gravity control".